Title

Temporal and spatial coordination of chromosome movement, spindle formation, and nuclear envelope breakdown during prometaphase in Drosophila melanogaster embryos.

Journal

The Journal of cell biology, 111(6 Pt 2)

ISSN

0021-9525

Authors

Hiraoka, Y
Agard, DA
Sedat, JW

Publication Date

1990-12-01

DOI

10.1083/jcb.111.6.2815

Peer reviewed

Temporal and Spatial Coordination of Chromosome Movement, Spindle Formation, and Nuclear Envelope Breakdown During Prometaphase in *Drosophila melanogaster* Embryos

Yasushi Hiraoka, David A. Agard, and John W. Sedat

Department of Biochemistry and Biophysics and the Howard Hughes Medical Institute, University of California, San Francisco, San Francisco, California 94143-0554

Abstract. The spatial and temporal dynamics of diploid chromosome organization, microtubule arrangement, and the state of the nuclear envelope have been analyzed in syncytial blastoderm embryos of *Drosophila melanogaster* during the transition from prophase to metaphase, by three-dimensional optical sectioning microscopy. Time-lapse, three-dimensional data recorded in living embryos revealed that congression of chromosomes (the process whereby chromosomes move to form the metaphase plate) at prometaphase occurs as a wave, starting at the top of the nucleus near the embryo surface and proceeding through the nucleus to the bottom. The time-lapse analysis was augmented by a high-resolution analysis of fixed embryos where it was possible to unambiguously trace the three-dimensional paths of individual chromosomes. In prophase, the centromeres were found to be clustered at the top of the nucleus while the telomeres were situated at the bottom of the nucleus or towards the embryo interior. This polarized centromere–telomere orientation, perpendicular to the embryo surface, was preserved during the process of prometaphase chromosome congression. Correspondingly, breakdown of the nuclear envelope started at the top of the nucleus with the mitotic spindle being formed at the positions of the partial breakdown of the nuclear envelope. Our observations provide an example in which nuclear structures are spatially organized and their functions are locally and coordinately controlled in three dimensions.

MITOSIS requires a precise coordination of cytoplasmic and nuclear events: chromosome condensation, fragmentation of the endoplasmic reticulum, vesicularization of the Golgi apparatus, nuclear envelope breakdown, spindle formation, chromosome segregation, and reformation of the nuclear envelope. Control mechanisms involved in the initiation of mitosis have been extensively studied genetically and biochemically (reviewed in Nurse, 1990). These lead to dramatic changes in phosphorylation of a number of proteins including histones and lamins; for example, chromosome condensation is accompanied by phosphorylation of histone H1 and H3 (Matthews and Bradbury, 1978; Gurley et al., 1978), nuclear envelope breakdown is likely to be caused by phosphorylation of lamins (Ward and Kirschner, 1990; Heald and McKeon, 1990; Peter et al., 1990), and phosphorylation of centrosomes increases their microtubule-organizing capacity (Vandré and Borisy, 1985). It remains to determine the temporal and spatial relationships of these events to build a complete picture of this dynamic process. In this paper, we have analyzed the dynamics of the three-dimensional arrangement of chromosomes within the nucleus and have sought to relate the observed spatial patterns to the dynamics of the nuclear envelope and microtubule organization during the prometaphase transition. A key aspect of this work has been the three-dimensional microscopic examination of individual nuclei, which provides the unique capability of directly visualizing transient, ephemeral structures, and interactions.

Early embryos of *Drosophila melanogaster* provide a powerful system for studying dynamic aspects of the mitotic cycle. In the first 13 nuclear cycles of *Drosophila* embryos, nuclei divide every 10–20 min (Zalokar and Erk, 1976). At late syncytial blastoderm stage from nuclear cycles 10–13, nuclei form a monolayer on the embryo surface, providing as many as 5,000 geometrically related examples of nuclear structures in a single embryo. Nuclear divisions are essentially synchronous with a shallow gradient of mitotic stages along the length of the embryo (Foe and Alberts, 1983). This gradient allows the time dependence of the chromosome arrangement to be examined by simply viewing closely spaced nuclei in a single fixed embryo. Another advantage of *Drosophila* is that a number of mutations affecting chromosome structure and mitosis during these stages of embryogenesis have been obtained (reviewed in Glover, 1989). In addition, the small number of chromosomes ($2\ n = 8$) simplifies the identification of chromosomes and the analysis of their spatial relationships.

Until recently, it has only been possible to examine the

nondisrupted, three-dimensional arrangement of chromosomes in certain specialized tissues containing polytenized giant chromosomes such as salivary gland nuclei in *Drosophila melanogaster* (Mathog et al., 1984; Hochstrasser et al., 1986). By contrast, in diploid tissues, chromosome arrangement has been studied mostly using squash preparations of chromosomes and statistical models to infer their three-dimensional arrangement (reviewed in Avivi and Feldman, 1980). The major difficulty associated with the direct examination of diploid chromosomes was their considerably smaller size. *Drosophila* diploid chromosomes (with widths of 0.2–0.4 μm in the condensed states) are packed in a nucleus of 4–5 μm diameter. In dramatic contrast, the diameter of a polytene nucleus is 30 μm and each polytene chromosome has a width of 3 μm. Thus, an increase of nearly an order of magnitude in resolution over that obtained for the studies on polytene chromosomes was required to examine diploid chromosomes.

Recent technological developments in light microscopy, using computational image processing (reviewed in Agard et al., 1989; Fay et al., 1989) or confocal microscopes (reviewed in Brakenhoff et al., 1989) to remove out-of-focus image information, have made it possible to examine the three-dimensional organization of diploid chromosomes directly in intact cells (Agard et al., 1988; Rawlins and Shaw, 1988; Oud et al., 1989). Unfortunately, currently available confocal microscopes have proved to be too insensitive to record useful three-dimensional data for the very small *Drosophila* embryonic chromosomes. Thus, in our procedures, three-dimensional microscopic images are recorded on a cooled, charge-coupled device (CCD)[1] using an ordinary fluorescence microscope (Hiraoka et al., 1987; Aikens et al., 1989) and the out-of-focus image information is computationally removed (Agard et al., 1989). Furthermore, using the computational approach it is now possible to examine living samples in three dimensions by time-lapse, optical sectioning microscopy (Minden et al., 1989; Hiraoka et al., 1989).

In this report, we describe the evolution of the spatial organization of chromosomes during the transition from prophase to metaphase and their interactions with nuclear envelope and mitotic spindle in *Drosophila* syncytial blastoderm embryos. This was accomplished by three-dimensional, optical sectioning microscopy, using both time-lapse optical sectioning of nuclei in living embryos and high-resolution optical sectioning in fixed embryos. The time-lapse recording scheme allows analysis of the dynamic behavior of chromosomes in individual nuclei as a function of time. This was augmented by the high-resolution analysis in fixed embryos where the exact locations of the centromeres and telomeres can be determined and the individual chromosome arms traced in three dimensions and uniquely identified. The spatial relationships among chromosomes, microtubules, and the nuclear envelope were examined by simultaneous observation of multiple cellular components in three dimensions. Our results revealed that in blastoderm stage embryos, prophase and metaphase chromosomes have a geometrically polarized arrangement relative to the embryo surface, and that this polarized arrangement is preserved during prometaphase chromosome congression (the process whereby chromosomes move together and pack tightly to form the metaphase plate). Importantly, prometaphase chromosome congression, nuclear envelope breakdown, and mitotic spindle formation all take place in a polarized fashion starting near the embryo surface. An implication of our observations is that prometaphase chromosome congression, nuclear envelope breakdown, and mitotic spindle formation are locally regulated and that the three-dimensional, spatial organization of nuclear structures is important for the coordination of their functions.

1. *Abbreviations used in this paper*: CCD, charge-coupled device; DAPI, 4',6-diamidino-2-phenylindole.

Materials and Methods

Microscope System Description

Two CCD microscope systems were used for data collection. (*a*) A liquid nitrogen-cooled CCD camera (Photometrics, Ltd., Tucson, AZ) with a 640 × 1,024 pixel CCD chip (RCA) is coupled to a Zeiss inverted Axiomat microscope; microscope lamp shutter, focus movement, and CCD data collection are controlled by a VAX 8650 computer (Hiraoka et al., 1987). (*b*) A Peltier-cooled CCD camera (Photometrics, Ltd.) with a 1,340 × 1,037 pixel CCD chip (Kodak-Videk) is coupled to an Olympus inverted microscope IMT-2; microscope lamp shutter, focus movement, CCD data collection, and filter combinations are controlled by a MicroVax III workstation (Minden et al., 1989; Hiraoka et al., 1989).

Optical Sectioning Microscopy of Chromosomes in Living Embryos

Rhodamine-labeled calf thymus histones H2A and H2B (a gift of Dr. J. S. Minden) were microinjected to *Drosophila* embryos 30 min after oviposition. The injected histones are incorporated into chromosomes during the periods of DNA replication and allow visualization of chromosomes in the living state during several mitotic cycles. Embryos injected with histones and observed under the microscope develop normally to hatching. The details of the methods are described in Minden et al. (1989).

The embryos were illuminated with a 100 W mercury arc lamp attenuated 20-fold and observed on the Olympus IMT-2 microscope using an Olympus oil immersion objective lens (40×; NA = 1.3) and a high selectivity rhodamine filter combination (Omega Optical, Inc., Brattleboro, VT). The CCD pixel size corresponds to 0.17 μm in the specimen plane. To speed up image readout, images were taken on a small portion of the CCD, 256 × 256 pixels corresponding to a 44 × 44 μm area. Five optical section images were taken by stepping the microscope focus in increments of 1 μm with an exposure time of 0.1 s. It took 5 s to read out each image; thus, 25 s for one cycle of a focus series. This was repeated continuously as a time course.

Optical Sectioning Microscopy of Chromosomes in Fixed Embryos

Drosophila embryos were fixed with 3.7% formaldehyde (freshly prepared from paraformaldehyde) in a 1:1 mixture of heptane/buffer A (15 mM Pipes pH 7.0, 80 mM KCl, 20 mM NaCl, 0.5 mM EGTA, 2 mM EDTA, 0.5 mM spermidine, 0.2 mM spermine, 0.1% 2-mercaptoethanol); chorion and vitelline membrane were removed as described previously (Mitchison and Sedat, 1983). The embryos were stained with 0.1 μg/ml 4',6-diamidino-2-phenylindole (DAPI) and examined on a Zeiss Universal microscope to determine their developmental stage from the density of nuclei on embryo surface (Foe and Alberts, 1983). The selected embryos were attached to a glass slide by adhesion to poly-L-lysine and mounted in buffer A as a immersion medium without coverslip. For high-resolution imaging of chromosomes, optical section images were collected on the CCD at focus step of 0.2 or 0.25 μm using a Zeiss water immersion coverslip-free objective lens (63×; NA = 1.2) on a Zeiss Axiomat microscope. The CCD pixel size corresponds to 0.070 μm in the specimen plane.

Indirect Immunofluorescence and Optical Sectioning Microscopy of Triply Stained Embryos

For indirect immunofluorescence microscopy, embryos were prepared as

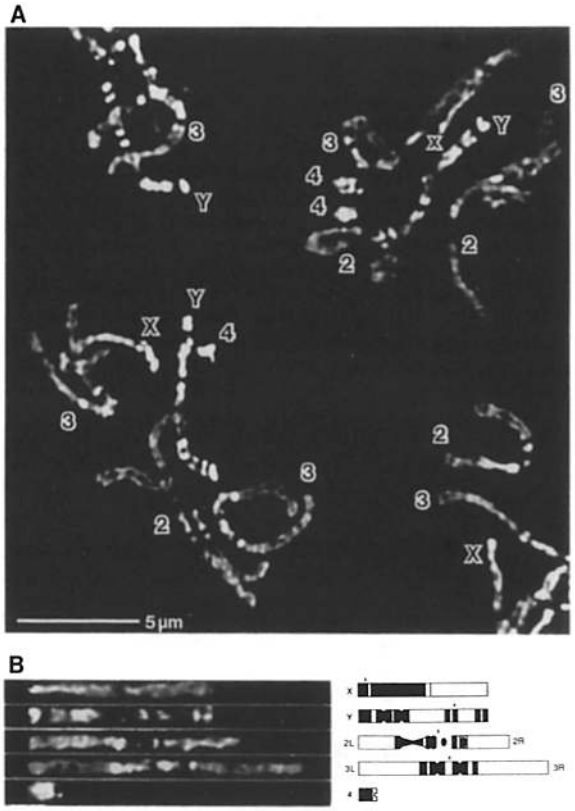

Figure 1. A cytological map of DAPI-staining patterns. (*A*) Squash preparation of chromosomes from a male embryo stained with DAPI. (*B*) Computationally straightened chromosomes (*left*) and diagram of DAPI-staining patterns (*right*). In the diagram, dark regions represent bright fluorescence in DAPI staining; short vertical bars represent the position of centromere.

described above but with one modification; taxol (10 μl of a 0.5 mM solution in dimethylsulfoxide) was added to the fixation mixture (5 ml of heptane and 5 ml of buffer A containing 3.7% formaldehyde) to stabilize microtubules (Karr and Alberts, 1986). Antibody staining was carried out as described previously (Fuchs et al., 1983) in a 96-well microtiter plate. Whole fixed embryos were incubated with PBT (PBS/0.1% Triton X-100) containing 10% normal goat serum, and then incubated with a mouse monoclonal antibody against *Drosophila melanogaster* lamin, B9 (Kuo et al., 1982) and a rat monoclonal antibody against yeast α-tubulin, YL1/2 (Kilmartin et al., 1982; Accurate Chemical & Scientific Corp., Westbury, NY) in PBT. Locations of lamin and tubulin were detected by incubation of these embryos with rhodamine-conjugated goat anti-mouse IgG (with minimal cross-reaction to rat serum proteins; Jackson Immuno Research Laboratories, Avondale, PA) and fluorescein-conjugated goat anti-rat IgG (with minimal cross-reaction to mouse serum proteins; Jackson Immuno Research Laboratories) in PBT containing 10% normal goat serum. The embryos were mounted in buffer A containing 0.1 μg/ml DAPI. The triply stained embryos were observed on the Olympus IMT-2 microscope using an Olympus oil immersion objective lens (60×; NA = 1.3). The CCD pixel size corresponds to 0.11 μm in the specimen plane. Optical section data were collected on the CCD at 0.2-μm focus intervals by repeating the following sequence at each focal plane. Three images were obtained sequentially for chromosomes (DAPI), microtubules (fluorescein), and nuclear envelope (rhodamine), and then microscope focus was stepped by 0.2 μm. High selectivity excitation and barrier filter combinations (Omega Optical, Inc.) for DAPI, fluorescein, and Texas red were used (Texas red filter combination was used for rhodamine-labeled specimens). For wavelength switching during data collection, excitation and barrier filters are mounted on wheels rotated by a microstepping motor controlled by the Micro VAX. A single dichroic mirror with triple-band pass properties (Omega Optical, Inc.) designed for wavelengths of DAPI, fluorescein, and Texas red was used to eliminate significant image displacement during the wavelength switching, thus allowing the triple-color images to be superimposed without further alignment (the residual translational displacement was estimated using multicolor fluorescent beads under the observation conditions; x, y, and z displacements are 0.023, 0.062, and 0.084 μm, respectively, between DAPI and Texas red images, and 0.292, 0.131, and 0.285 μm, respectively, between DAPI and fluorescein images).

Image Processing and Analysis

Image processing and analysis are carried out on a VAX8650 computer or attached FPS 264 array processor (Floating Point Systems, Inc., Beaverton, OR) using programs written in Fortran. The out-of-focus information was removed by a three-dimensional iterative, deconvolution method with a non-negativity constraint (Agard et al., 1989) using the optical transfer function experimentally determined for the objective lens used (Hiraoka et al., 1990). Unlike subtractive methods such as the nearest neighbor deblurring method appropriate for larger biological structures (Agard and Sedat, 1983; Agard, 1984), this approach effectively moves the out-of-focus photons back to their correct positions within the object, thereby maintaining a high signal-to-noise ratio. By using current computer technology, three-dimensional deconvolution (25 iterations) can be performed in 1–2 h for a 512 × 512 × 64 pixel image. Images were further processed, as necessary, to enhance local contrast (Belmont et al., 1987), or to detect chromosome boundaries based on the three-dimensional intensity gradient (Chen et al., 1989).

An interactive modeling program to trace chromosome paths in a three-dimensional data stack is based on an earlier implementation (Mathog, 1985). Details of the computer algorithms are described in Chen et al. (1989). This program can open up to eight windows on a display screen at one time and display computationally rotated multiple views of the same object in each window. Chromosome paths are traced by a cursor and recorded as sets of three-dimensional coordinates, while the multiple images from various view angles are updated simultaneously to follow the cursor movement. Modeling and image display are carried out on a Parallax model 1280 graphic display with a 12 Mbyte image memory (Parallax Graphics Inc., Santa Clara, CA).

Software for computational manipulation of grey level information associated with traced chromosome paths to straighten or dissect the chromosomes has been developed. Grey level information associated with the selected chromosome paths is discriminated by thresholding the grey level intensity and/or detecting chromosome edges based on the intensity gradient, and dissected from the rest of chromosomes. The dissected chromosomes are recomposed as the outlines filled with a particular color. Each traced chromosome can be computationally straightened by a combination of operations of rotation, translation and transformation based on the three-dimensional geometry.

Identification of Chromosomes

Drosophila melanogaster has two sets of four chromosomes (X(Y), 2, 3, and 4) that can be identified by their shapes and DAPI-staining patterns. Chromosome 4 is the smallest and is recognized as a tiny bright spot; chromosomes 2 and 3 are metacentric and each arm is shorter than that of sex chromosomes X and Y, which are telocentric and acrocentric, respectively. Thus, 10 chromosome arms should be recognized in a diploid nucleus (two sets of X(Y), 2L, 2R, 3L and 3R; chromosome 4 and the short arm of chromosome Y are ignored). The Y chromosome is the most distinctive with its bright heterochromatic blocks along the entire chromosome. Although the euchromatic arms of chromosomes 2 and 3 have relatively few distinctive features, these chromosomes can be distinguished from one another by the heterochromatic blocks near the centromere. These features were deduced from spread chromosome preparations (Fig. 1); similar results have been previously reported (Kaufmann, 1934; Holmquist, 1975; Gatti et al., 1976; Halfer, 1981; Gatti and Pimpinelli, 1983).

Results

We examined three-dimensional nuclear structures in *Drosophila melanogaster* embryos specifically at nuclear cycles 12 and 13 while nuclei divide rapidly and essentially synchronously. Nuclei were viewed from a direction perpendicular to the embryo surface; thus microscopic images are approximately parallel to the embryo surface unless described otherwise. In this report, the "top" of a nucleus refers to loca-

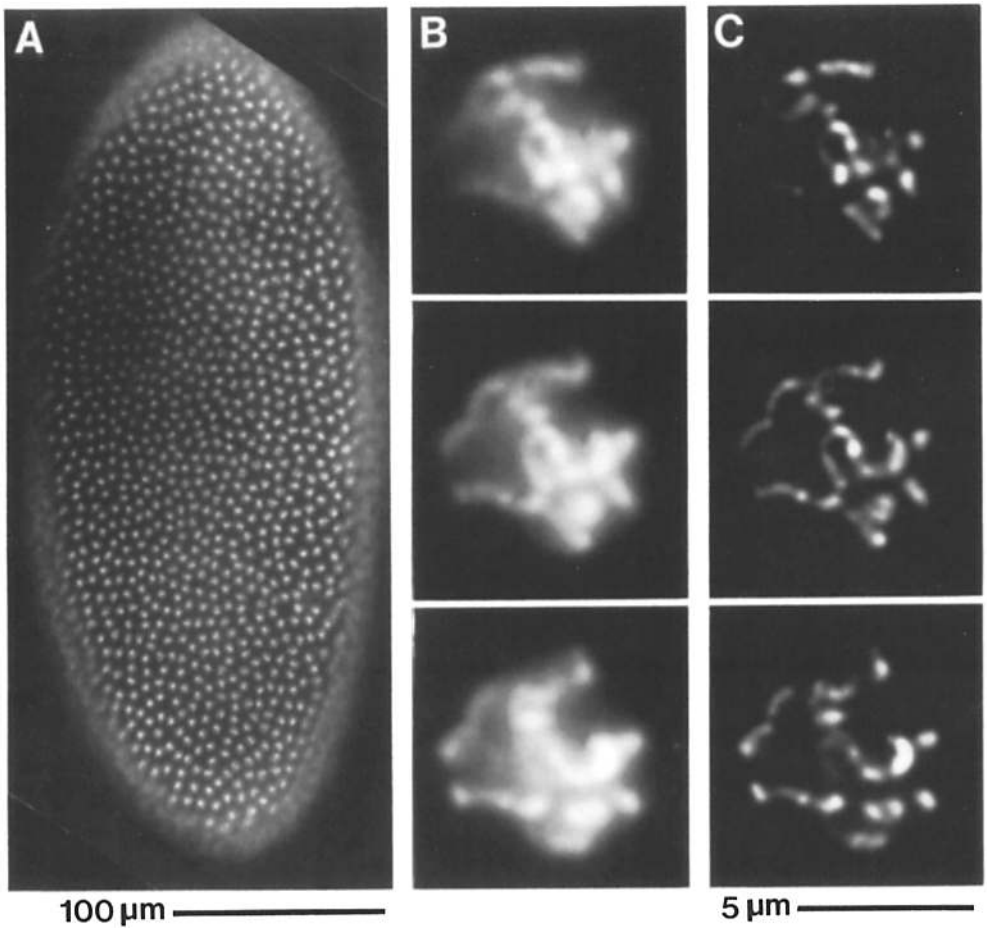

Figure 2. Optical sectioning and image processing of embryonic nuclei. Low magnification view (*A*) of a whole embryo stained with a DNA-specific fluorescent dye, DAPI. Every bright spot distributed throughout the embryo surface represents a single individual nucleus. An example of optical sections from a three-dimensional data stack before (*B*) and after (*C*) the removal of out-of-focus image contamination. Three-dimensional image data were obtained at 0.25-μm focus intervals under computer control. Each displayed section is separated by 0.5 μm in the focus (*z*) direction. The out-of-focus information was removed by an iterative deconvolution method with a nonnegativity constraint (Agard et al., 1989) using the optical transfer function experimentally determined for the objective lens used (Hiraoka et al., 1990).

tions near the embryo surface whereas the "bottom" refers to locations toward the embryo interior.

Determination of Chromosome Arrangement Within a Diploid Nucleus

Three-dimensional data were collected as a series of images recorded at different focal planes by stepping the microscope focus. For the high-resolution analysis of chromosome organization in fixed specimens, optical section images were taken at 0.2–0.25-μm focus intervals and computationally processed to remove out-of-focus image information as described in Materials and Methods. An example of such optical sectioning of diploid prophase nuclei in fixed embryos is shown in Fig. 2. Fig. 2 *A* shows an entire *Drosophila* embryo prepared and fixed under conditions previously shown to preserve chromosome structure by electron microscopy (Belmont et al., 1989) and stained with the nonintercalative DNA-specific fluorescent dye, DAPI. Optical sections, before and after the image processing, are shown in Fig. 2, *B* and *C*, respectively. The image processing employed here, three-dimensional iterative, constrained deconvolution, acts to improve the microscopic resolution by recovering an estimate of the true object from the observed microscopic image using knowledge of the microscope's point-spread function, or a smearing function (for a discussion of mathematical basis of this method, see Agard et al., 1989; also see Materials and Methods). To trace the paths of chromosomes in an embryonic diploid nucleus, image processing of this type is absolutely essential, because an embryonic diploid nucleus is so small that the point spread function covers almost the entire nucleus. Note that chromosome strands barely resolved in the original image are clearly resolved following image processing (Fig. 2, *B* and *C*).

The processed three-dimensional data were analyzed to determine the spatial arrangement of chromosomes within the nucleus. First, paths of chromosomes were traced in three dimensions using interactive computer software optimized for examining complex biological images (Chen et al., 1989; also see Materials and Methods). Once chromosome paths were determined, a computational dissection scheme was used to visualize the structural features of the chromosomes (see Materials and Methods). Second, the traced paths were identified as belonging to particular chromosomes by their characteristic DAPI-staining patterns and also by their shapes. To accomplish this, a cytological map of DAPI-staining patterns for diploid chromosomes was made from spread chromosome preparations that were fixed and stained under the conditions used for the three-dimensional analysis (see Fig. 1 in Materials and Methods).

An example of a model representing the traced three-dimensional paths of the chromosomes is shown in Fig. 3. Fig. 3 *A* shows a projected view of a diploid prophase nucleus reconstructed from the processed optical section data presented in Fig. 2 *C*. Models of chromosome paths that

were traced and identified are shown in Fig. 3, *B* and *C*, in top and side views, respectively. All of the chromosomes were identified (X, Y, 2, 3 and 4) and each is presented using a different color. Centromeres and telomeres are marked by closed and open circles, respectively. To aid in the examination of chromosome organization, the modeled paths can be used as a guide to computationally dissect the chromosomes from within the prophase nucleus (Fig. 3 *D*) and to then reconstruct the nucleus with each chromosome appropriately colored (Fig. 3 *E*, compare with Fig. 3 *A*). Note specifically that the configuration of the third chromosomes, obscured in the projected view by the remaining chromosomes, can be clearly seen in the dissected view. These capabilities of modelling greatly facilitated the interpretations described in the next section.

Spatial Arrangement of Chromosomes in Prophase Nuclei

Chromosome paths were traced for 13 prophase nuclei. These nuclei shared several common features. The nucleus presented in Fig. 3 represents a typical example of late prophase nuclei. Two homologous sets of chromosomes can be clearly seen, indicating that homologous chromosomes are not synapsed (Fig. 3, *B* and *D*). Centromeres were found to cluster along a line as indicated by arrow heads in Fig. 3 *B*. Based on observations from the living data (see Fig. 4 *A* below), this line forms what will later become the axis of metaphase plate. Examined from the top, the arrangement of chromosomes seems to be roughly spherical in shape (Fig. 3 *B*). However, when examined in a side view from the direction of the centromere line-up, the very early stage of chromosome congression in the top portion of nucleus can be seen as an indentation (shown by *arrows* in Fig. 3 *C*).

By using the side view of the model (Fig. 3 *C*), it can be clearly seen that the centromeres are located in the top half of the nucleus near the embryos surface (top of the figure), the telomeres in the bottom half of the nucleus, and that the chromosome arms are oriented approximately perpendicular to the embryo surface. This polarized centromere–telomere orientation of autosomal as well as sex chromosomes perpendicular to the embryo surface was observed in all the prophase nuclei examined.

It is also clear from the data (Fig. 3, *B–D*) that telomeres of homologous chromosomes are closely associated at the bottom of the nucleus (indicated by *asterisk* in Fig. 3 *D*). In this nucleus, all four telomeres of the third chromosomes are near each other, with two of them touching each other; the telomeres of one arm of the second chromosomes are also associated. Association of telomeres was commonly observed in prophase nuclei, often making it difficult to detect the precise ends of individual chromosomes.

The total length of the prophase chromosomes contained within a nucleus ranged from 64 to 78 μm (average 70 $\pm$ 6 μm for 13 examples) as expected for two separate sets of chromosomes (Holmquist, 1975; Halfer, 1981; Pimpinelli et al., 1976). This provides a further indication that homologous chromosomes are not synapsed.

Prometaphase Chromosome Congression Takes Place in a Polarized Fashion Starting at the Top of the Nucleus

To examine how prophase chromosomes change their three-dimensional arrangement as they approach metaphase, we followed chromosomes in the living state. Chromosomes in living *Drosophila* embryos were visualized by microinjection of fluorescently labeled histones that are subsequently incorporated into newly replicated chromatin (Minden et al., 1989; Hiraoka et al., 1989). Owing to temporal constraints caused by the very rapid mitotic cycle, optical section data were taken on the CCD at five focal planes spanning the nucleus with a 1-μm focus step every 5 s. Such three-dimensional data sets were collected as a function of time to make a time-lapse series of optical section data.

Fig. 4 *A* shows, for a single nucleus, the morphological changes occurring from prophase to metaphase displayed as a focus series (left to right represents the progression from the bottom to top of the nucleus) and as a time course (shown vertically; time to the metaphase/anaphase transition is represented with the negative sign). Based on this data, formation of the metaphase plate (visualized as a rectangular shape) can be seen to initiate at the top of the nucleus, and to progress from top to bottom by the passage through the nucleus of a smooth wave of chromosome congression (indicated by *asterisks* in Fig. 4 *A*).

This process of chromosome congression was quantified by measuring the ellipticity of chromosome figures at different focal planes as a function of time. The width measured in the short axis was normalized to the length along the long axis, where the long axis (*L*) was defined by the direction of metaphase plate and the short axis (*S*) was defined to be perpendicular to the long axis (see Fig. 4 *A*). This ratio of the short axis to the long axis (S/L) was measured at three focal planes, each separated by 2 μm. The ratio is 1 for the spherical morphology occurring in prophase and decreases toward metaphase. The ratio was averaged over 14 nuclei and plotted for each focal plane as a function of time (Fig. 4 *E*), together with examples for three individual nuclei (Fig. 4, *B–D*). This shows that the width of chromosome figures decreases earlier at the top of the nucleus than at bottom. This differential behavior of chromosome congression is not a result of the time-lapse interval, as the 5-s delay per section was taken into consideration in the plotting.

By using the averaged data shown in Fig. 4 *E* the speed of the wave of congression can be estimated. It takes the wave 2 min to travel the 4 μm from the top to the bottom of the nucleus or 2 μm/min. Note that at this developmental stage the duration of the mitotic cycle is 22 min. Once the wave reaches the bottom of the nucleus, formation of the metaphase plate is complete. Chromosomes then remain on the metaphase plate for an additional 3 min before separating in anaphase. During this period, chromosomes are making elastic motions, or swaying, inside the metaphase plate.

The Polarized Arrangement of Chromosomes Is Maintained During the Process of Metaphase Plate Formation

To analyze the detailed arrangement of chromosomes from prophase to metaphase, fixed preparations were examined. The same overall three-dimensional nuclear morphology observed in living embryos was also seen in fixed embryos. Fig. 5 shows a portion of a fixed embryo, displayed as a focus series. By comparison with the living preparation shown in Fig. 4 *A*, it can be seen that a series of nuclei of gradually

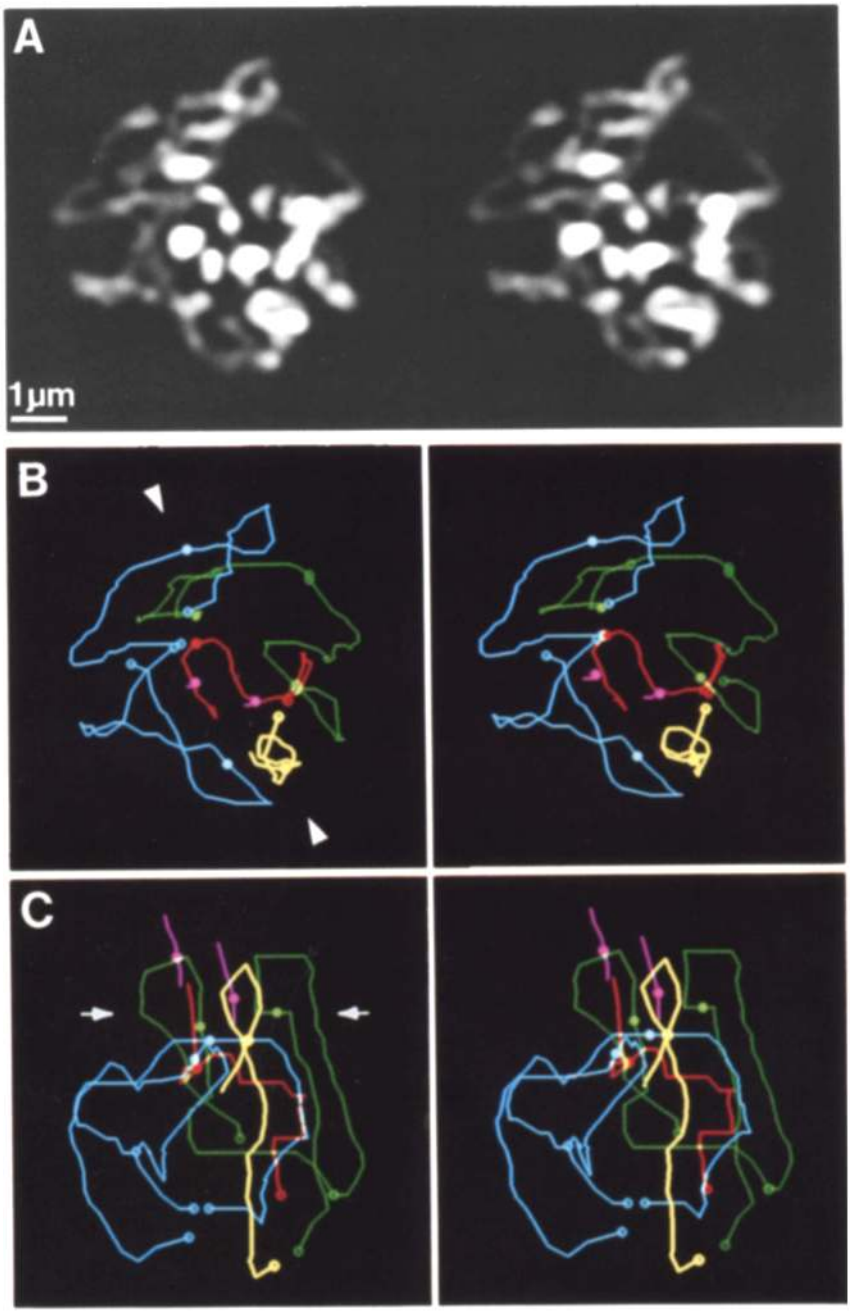

Figure 3. Stereo model for prophase chromosome arrangement. (*A*) Stereo projection was made from 32 optical section images, each separated by 0.25 μm, of the nucleus (Fig. 2 *C*) after image processing. (*B*) A model made by tracing chromosome paths. (*C*) Side view of the same model viewed from the direction shown by the arrowheads in (*B*). In the side view, the embryo surface is on the upper side of the figure. Color for chromosome: X, *yellow*; Y, *red*; 2, *green*; 3, *blue*; 4, *purple*. Closed and open circles represent centromeres and telomeres, respectively. (*D*) Chromosomes were computationally dissected by isolating cylinders surrounding the traced paths. Dissected from the prophase nucleus shown in *A*. Telomeric association is shown by asterisk. Arrowhead represents centromere. Arrows on third chromosomes indicate the bending of chromosomes at homologous sites. (*E*) Recomposed from the dissected individual chromosomes with pseudocolor for each chromosome.

changing morphology were spaced along the mitotic gradient in a single embryo (in this example, nuclei at the right initiated mitosis earlier). The nuclear structures at the left show a spherical appearance at the bottom (inside the embryo) but show a rectangular shape at the top (near the embryo surface), whereas nuclei to the right show a nearly rectangular shape throughout the entire focal series.

The spatial arrangement of chromosomes was analyzed in these early metaphase plates (12 examples examined). Fig. 6 shows an example of a reconstruction of chromosomes in the metaphase plate indicated by the arrow in Fig. 5. In metaphase, unlike in prophase, the telomeres were not associated, resulting in complete separation of homologous chromosomes; all the expected 10 telomeres (two sets of X(Y), 2L, 2R, 3L and 3R; see Materials and Methods) were clearly detected at the bottom of the metaphase plate as shown in Fig. 6 *A*. Starting at the telomeres, the three-dimensional paths of all the 10 chromosome arms were traced up to the centromeres at the top of the metaphase plate (see Fig. 6, *B* and *C*; the numbers for chromosome arms in Fig. 6 *C* correspond to those for the telomeres in Fig. 6 *A*). Chromosome arms were oriented predominantly perpendicular to the embryo surface similar to those in prophase. This can be seen in a side view of a model for the traced chromosomes

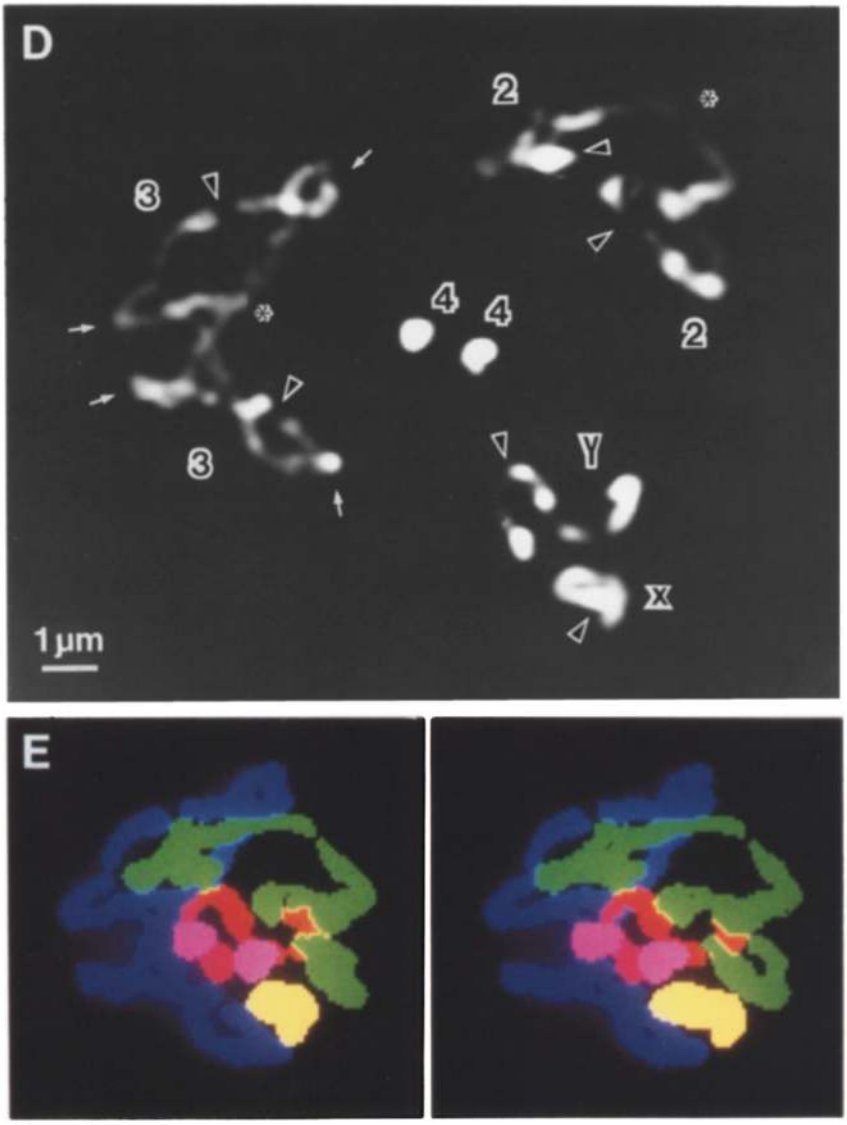

Figure 3.

(Fig. 6 *B*; compare with Fig. 3 *C*) and cross-section views of the metaphase plate (Fig. 6 *C*). In the sectional views, all 10 chromosome arms, running perpendicular to the embryo surface, can be seen as numbered in Fig. 6 *C*.

Due to the intrinsic properties of microscopic image formation, the microscopic resolution along the optical axis is relatively lower than that in the microscope field plane (for detailed discussion, see Agard, 1984). Since we are viewing embryos from a direction perpendicular to the embryo surface, we wished to test whether the polarized orientation of chromosomes perpendicular to the embryo surface was an artificial result of the viewing direction. To eliminate this possibility, we examined chromosome organization in an edge view of embryos that were cut in half by a razor blade. Consistent results were obtained from this viewing direction as well. In this view, chromosome arms mostly fit within an image plane, running from the surface to inside the embryo with centromeres localized near the embryo surface (data not shown).

The Nuclear Envelope Breaks Down Differentially, Initiating at the Position of Mitotic Spindle Formation at the Top of the Nucleus

To examine the involvement of microtubules and the nuclear envelope in the process of chromosome congression, we observed microtubules and the nuclear envelope at the prometaphase transition. Whole-mount embryos were fixed and fluorescently stained using well-characterized, antitubulin and antilamin antibodies. Microscopic images for each of three fluorescent stainings for chromosomes, microtubules, and nuclear envelope were obtained sequentially in the same field and at the same focal plane. This was repeated at 0.2-μm focus intervals to make a set of aligned, triple-color, three-dimensional image data as described in Materials and Methods.

As shown in Fig. 7, the chromosomes again showed the arrangement typical of prometaphase, that is, a spherical appearance at the bottom and a rectangular shape at the top

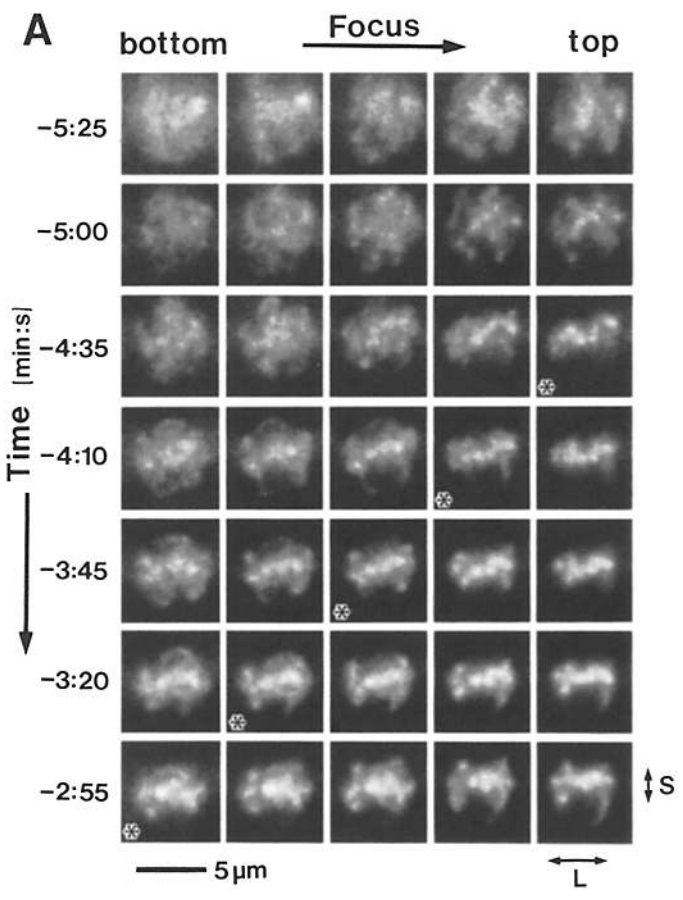

Figure 4. Optical sectioning of chromosomes in a living embryo. (*A*) Single nucleus is displayed as a focus series (*left to right*) and as a time course (*top to bottom*). Optical section was taken at 1-μm focus interval from bottom (inside the embryo) to top (near the embryo surface) of the nucleus. The top portion of the nucleus (*right side*) was packed earlier than the bottom portion (*left side*). Numbers on the left represent time to the metaphase-anaphase transition in minutes:seconds with the negative sign. (*B–E*) Width of chromosome figures at different focal planes. Ratios of the short axis to the long axis of a chromosome figure (*S/L*) at three focus planes are plotted as a function of time, for three individual nuclei (*B*, *C*, and *D*) and for the average of 14 nuclei (*E*). Time is represented to the metaphase-anaphase transition in minutes with the negative sign. Top (■); middle (○); bottom (□).

(Fig. 7 *A*). Mitotic spindles were observed at the top, on both sides of the rectangular array of centromeres (the top panel in Fig. 7 *B*). The nuclear envelope remained spherical for the bottom half of the nucleus although it looked somewhat fragmented (the bottom two panels in Fig. 7 *C*), whereas the top portion of nuclear envelope had already broken down (the top panel in Fig. 7 *C*). Regions of partial breakdown of the nuclear envelope are indicated by arrows in Fig. 7 *C*. Interphase embryos fixed and stained under the identical conditions have an intact nuclear envelope (data not shown, and also Fuchs et al., 1983; Paddy et al., 1990).

Fig. 8 shows superimposed images of chromosomes, microtubules, and nuclear envelope. In this figure, the spatial relationships of these three structures can be seen. The positions of the partial nuclear envelope breakdown correspond to the location of the mitotic spindle (*arrows* in Fig. 8). Significantly, close location of chromosomes to the nuclear envelope, with an indication of attachment, can be seen at the bottom half of the nucleus (examples indicated by *arrowheads* in Fig. 8).

Discussion

We have analyzed the three-dimensional arrangement of chromosomes, the nuclear envelope, and microtubules from prophase to metaphase in *Drosophila melanogaster* syncytial blastoderm embryos. The arrangement of chromosomes was analyzed by three-dimensional, optical sectioning microscopy both in fixed and living embryos; their spatial relationships with microtubules and the nuclear envelope were examined by multiple-wavelength, optical sectioning microscopy in fixed preparations. The time-lapse optical sectioning of living embryos not only acts as an ideal control for possible artifacts in the fixed preparations but also provides the unique capability of observing the behavior of individual nuclei over time. On the other hand, the high-resolution optical sectioning in fixed embryos complements the living data recorded by necessity at lower spatial resolution. These approaches have allowed us to reexamine mitotic events, paying special attention to the role that three-dimensional organization plays in mitotic function. Our results have demonstrated that prometaphase chromosome congression takes place in a geometrically polarized fashion, progressing sequentially as a wave from the top to the bottom of the nucleus. Furthermore, such polarized behavior of the chromosomes is temporally and spatially coherent with mitotic spindle formation and nuclear envelope breakdown. The spatial and temporal patterns of chromosomes, mitotic spindles and the nuclear envelope occurring during the blastoderm stage embryonic mitoses are shown schematically in Fig. 9.

Arrangement of Chromosomes in Blastoderm Embryos

The polarized configuration of interphase chromosomes

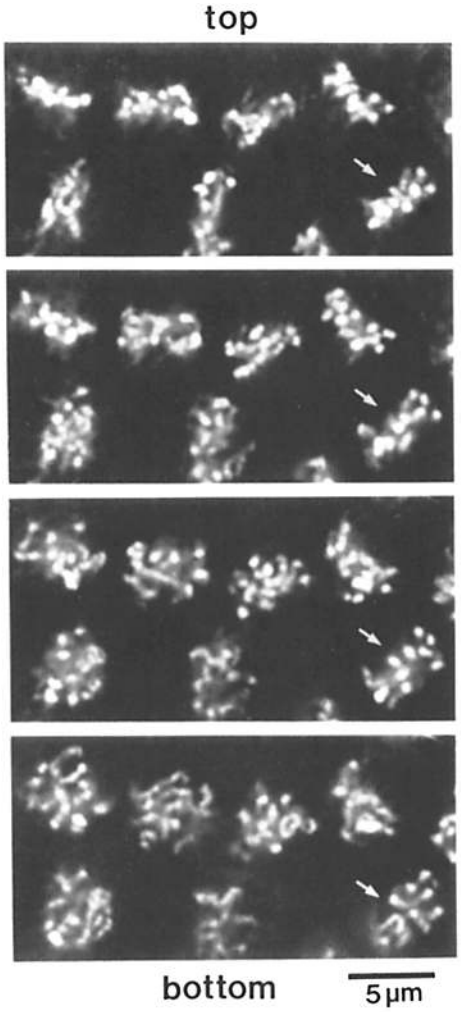

Figure 5. Mitotic gradient in a fixed embryo. A small portion of a fixed embryo stained with DAPI is shown at four focal planes, each separated 1 μm along the focus direction, from the interior (*bottom*) to the surface (*top*) of the embryo. In this example, the mitotic gradient started at the right and proceeded through to the left (nuclei at the right are more advanced in mitosis).

with centromeres and telomeres on each end of the nucleus has been inferred in a wide range of species (reviewed in Avivi and Feldman, 1980; Comming, 1980; Fussel, 1984), for example, by the use of laser irradiation of small regions of chromosomes (Cremer et al., 1982), or by radioactive labeling of late replication regions at centromeres and telomeres (Fussel, 1975). In *Drosophila melanogaster*, the polarized arrangement was demonstrated by directly tracing the three-dimensional paths of chromosomes within polytene nuclei (Mathog et al., 1984; Hochstrasser et al., 1986), or by using prematurely condensed chromosomes observed in oxygen-deprived embryos (Foe and Alberts, 1985). It should be noted that in syncytial blastoderm stage embryos, chromosomes are not only polarized but also have a defined geometrical orientation relative to the embryo surface. In interphase nuclei, centromeres are observed as several bright spots of centromeric heterochromatin clustered in a small region near the embryo surface (Foe and Alberts, 1985; for similar observations in *Drosophila virilis*, see Ellison and Howard, 1981). Correspondingly, asters of microtubules are formed and duplicated at the top of the nuclei near the embryo surface (Karr and Alberts, 1986).

We have shown here that this aligned configuration of chromosomes is preserved during the transition from prophase to metaphase (see Fig. 9). The metaphase plate is formed as a wave of chromosome compaction, progressing from centromeres to telomeres, preserving the positions of centromeres and telomeres relative to the embryo surface. Thus, in *Drosophila* embryos, metaphase chromosomes are polarized in a parallel arrangement with centromeres closest to the embryo surface, whereas those in other well-studied species are radially arranged with centromeres toward the center and telomeres toward the periphery of the metaphase plate (Chaly and Brown, 1988; Belmont et al., 1989). However in Kc cells, a cultured *Drosophila* cell line derived from embryos, chromosomes on the metaphase plate are radially arranged similarly to their mammalian counterparts (Swedlow, J. R., unpublished results). Therefore, the alignment of nuclear structures may be related to a cytoskeletal organization particular to blastoderm stage embryos and be important in the developmental process.

The polarized centromere–telomere arrangement is generally believed to be a relic of the configuration formed during anaphase chromosome movement. However, it is interesting to note that during the process of forming the metaphase plate, the combination of congression and condensation leaves the chromosomes straight and highly polarized. Hence it might be possible that polarization is developed and reinforced in both metaphase and anaphase, and subsequently carries over to interphase. It should also be noted that in anaphase, the centromere–telomere orientation is parallel to the embryo surface and must rotate to resume the interphase upright orientation (see Fig. 9). Observations of nuclear behavior in living embryos show that unevenly spaced, divided nuclei are shuffled by a cytoplasmic motion at the transition from telophase to interphase, and repositioned to an evenly spaced arrangement (Minden et al., 1989). It is likely that the nuclear rotation takes place in accompany with this extensive repositioning of the nuclei.

Our analysis of the chromosome paths shows that, with the exception of telomeric association during prophase, homologous chromosomes are distinctly separate from one another. Furthermore, our in situ hybridization experiments using a DNA probe for histone genes indicate that homologous chromosomes are also separate in interphase syncytial blastoderm embryos (Hiraoka, Y., S. J. Parmelee, M. C. Rykowski, D. A. Agard, and J. W. Sedat, manuscript in preparation). This apparently contradicts genetic experiments on transvection which suggest that homologous chromosomes are associated (Lewis, 1954; Green, 1959; Jack and Judd, 1979; Gelbart, 1982). This contradiction can be reconciled by hypothesizing that the formation of homologous chromosome association only occurs after the syncytial blastoderm stage. This interpretation is consistent with the fact that transvection has been, as yet, reported only in differentiated tissues (reviewed in Wu and Goldberg, 1989) and is supported by our observations of in situ hybridization for histone genes indicating that the association of homologous

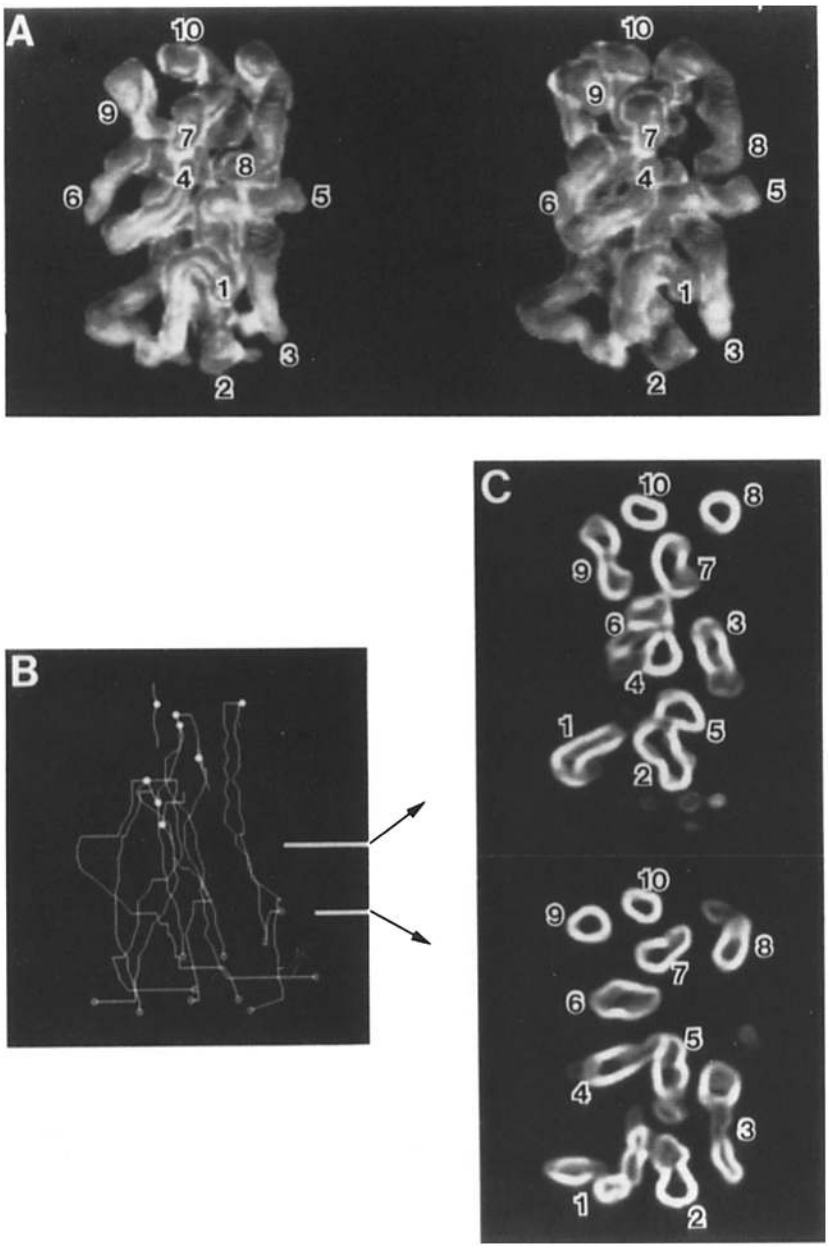

Figure 6. Chromosome arrangement in the metaphase plate. (*A*) Surface contour model in stereo. The model was constructed from the three-dimensional intensity gradient. It is viewed from the embryo interior. (*B*) Side view of a model for traced chromosome paths. In the side view, the embryo surface is on the upper side of the figure. (*C*) Cross-section views of metaphase plate at two different focal planes, separated by 2 μm, corresponding to the positions marked in *B*. The edges of chromosomes are displayed as the intensity gradient. Each chromosome arm is labeled by the same number in *A* and *C*.

chromosomes occurs before gastrulation (Hiraoka, Y., S. J. Parmelee, M. C. Rykowski, D. A. Agard, and J. W. Sedat, manuscript in preparation). During the syncytial blastoderm stage, synchronous mitotic cycles are driven by maternal stores of transcripts. Once embryos become cellularized, marked changes in patterns of gene expression are known to occur with the onset of differentiation (Anderson and Lengyel, 1979). This might be accompanied by changes of chromosome spatial organization.

The association of telomeres has been reported in a wide range of organisms (reviewed in Ashley and Wagenaar, 1974; Dancis and Holmquist, 1979). It is unknown whether this phenomenon is a direct consequence of the telomeric DNA sequences (Young et al., 1983; reviewed in Blackburn and Szostak, 1984; Zakian, 1989; Blackburn, 1990) or an indirect consequence of the tendency of telomeres to attach to the nuclear envelope (reviewed in Dancis and Holmquist, 1979; Holmquist and Dancis, 1979; Young et al., 1983; Hochstrasser et al., 1986). The fact that telomeres are separated in metaphase when the nuclear envelope disappears may support the latter case.

Coordination of the Polarized Events

Our ability to identify chromosomes and define their arrangement within the simple, monolayer geometry of synchronously dividing nuclei greatly facilitated the analysis of the spatial relationship between chromosomes and other cellular components at defined mitotic stages. We infer from our results that the initial congression of centromeres is

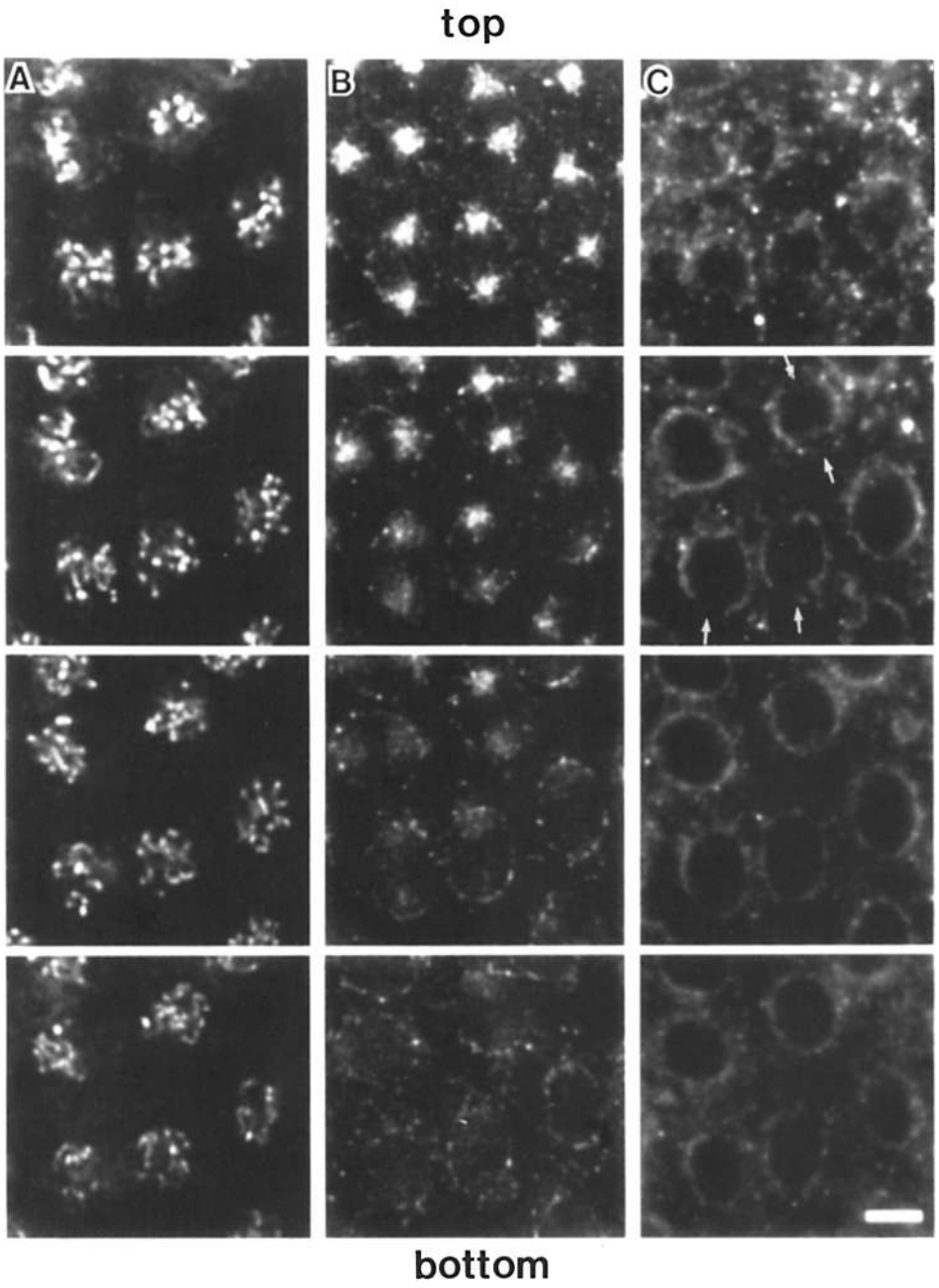

Figure 7. Optical sections of embryos triply stained for chromosomes, microtubules, and the nuclear envelope. Optical sections were obtained at 0.2-μm focus intervals. Selected optical sections are displayed for chromosomes (*A*), microtubules (*B*), and nuclear envelope (*C*) at four focal planes, each separated by 1 μm along the focus direction, from the interior (*bottom*) to the surface (*top*) of the embryo. Bar, 5 μm.

mediated by the mitotic spindle through the partially degraded nuclear envelope. (In earlier studies, the geometric changes associated with this initial stage of partial nuclear envelope breakdown had been recognized as an invagination of the nuclear envelope on both sides of the metaphase plate; Fuchs et al., 1983). At this stage, chromosomes in the bottom half of the nucleus appear to be still anchored onto the nuclear envelope, generating a characteristic shape with a spherical bottom and a rectangular top (for a schematic diagram, see Fig. 9). As chromosomes sequentially detach from the nuclear envelope, they move to pack into the metaphase plate. Although the majority of chromosome condensation has occurred during the period from interphase to prophase, chromosomes shorten by an additional 2-fold during prometaphase (Hiraoka, Y., unpublished results). This further condensation is generally considered to be distinct from the movement that defines congression. However, it is possible that chromosome condensation may provide the actual driving force that pull the chromosome arms onto the plate.

The geometrically polarized sequence of changes in nuclear structures observed during the process of prometaphase chromosome congression prompts us to hypothesize a wave of signals starting at the top of the nucleus and traveling through the nucleus to the bottom. The observed speed of this wave, 2 μm/min, is much too slow for a diffusion-

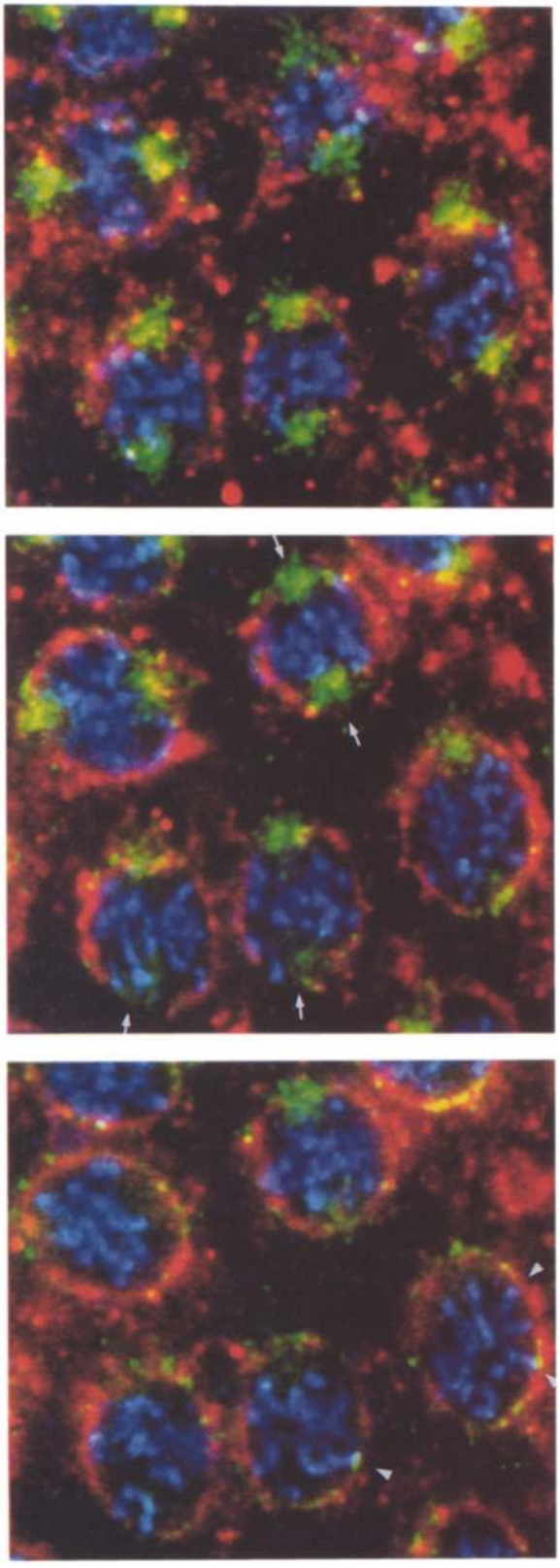

Figure 8. Superimposed images of chromosomes, microtubules, and the nuclear envelope. Chromosomes, microtubules, and nuclear envelope are displayed in *blue*, *green*, and *red*, respectively. The images were superimposed from the top three rows in Fig. 7.

mediated process (for the diffusion of dextran of various sizes in cytoplasm; see Luby-Phelps et al., 1986), and suggests that the signal may actually transit along structures such as microtubules or intermediate filaments. An interesting alternative is that the processes of chromosome congression and nuclear envelope breakdown may be processive, and that once initiated at the top of the nucleus, they both continue essentially independently until complete.

The fact that preferential breakdown of the nuclear envelope occurs just where the mitotic spindle is formed suggests that nuclear envelope breakdown and mitotic spindle formation are controlled locally and possibly by a common mechanism. Such a mechanism provides a reasonable candidate for initiating the wave. Because of its importance in regulating and coordinating mitotic cycle events, it is plausible that phosphorylation is involved in either the trigger or the propagated signal, or both. For example, both nuclear envelope breakdown and the microtubule-organizing capacity of centrosomes are likely to be regulated by phosphorylation (reviewed in Nurse, 1990). However, if phosphorylation were the key to the spatially-coordinated events described here, then one would expect to see a gradient of phosphorylation within a single nucleus, for which there is, as yet, no evidence.

It is unknown what molecular machines are required to maintain the geometrically-polarized organization of nuclear structures relative to the embryo surface, although it has been reported that changes in the organization of microtubules and actin filaments take place at the embryo cortex regions at the end of the nuclear cycle 9 when nuclei migrate to the embryo surface to form the monolayer (Karr and Alberts, 1986). Observations have been reported indicating that nuclei that fail nuclear division, as a result of mutations (Sullivan et al., 1990) or chromosomal cross-linking (Minden et al., 1989; Hiraoka et al., 1989) move to the embryo interior while normal nuclei remain at the surface. Moreover, the uncoupling of behaviors of nuclei and mitotic apparatus has been demonstrated in mutant embryos deficient of nuclear division (Freeman et al., 1986) or in embryos in which nuclear DNA replication had been blocked by an inhibitor to DNA polymerase α (Raff and Glover, 1988). In those cases, centrosomes continue their duplication and segregation without nuclear division or cytokinesis (Freeman et al., 1986; Raff and Glover, 1988; Sullivan et al., 1990).

Thus, it appears that there are mechanisms that engage nuclei in the proper position with the proper alignment, and that distinguish damaged nuclei and eliminate them from the developmental process. It is tempting to speculate that uncoupling of the well-coordinated nuclear processes results in the loss of the affected nuclei from the blastoderm layer. One implication of our observations is that the organized arrangement of chromosomes might facilitate coordinated interactions among chromosomes, mitotic apparatus, and the nuclear envelope to ensure the rapid and yet precise mitoses at the syncytial blastoderm stage.

We thank Dr. M. Gatti for providing his cytological maps of *Drosophila melanogaster* diploid chromosomes, Hans Chen for computer software development, Jonathan Minden for his help in microinjecting embryos, and Michael Paddy for his help in spread chromosome preparations. We also thank Mary Rykowski, Hirohisa Masuda, Tokuko Haraguchi, and Elizabeth Blackburn for critical reading of the manuscripts.

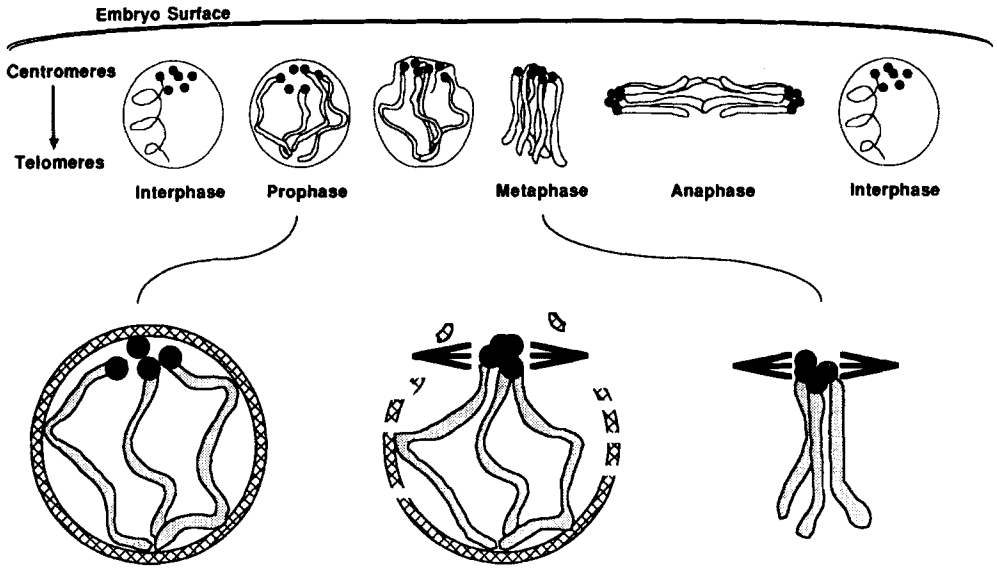

Figure 9. Spatial arrangement of embryonic chromosomes in the mitotic cycle. Chromosome arrangement during the mitotic cycle is shown relative to embryo surface. From interphase to metaphase, centromeres are situated at one side of the nucleus near the embryo surface and telomeres at the other side. Metaphase plate is formed as a wave from the top to the bottom side. During the process of anaphase chromosome separation, chromosome arms are oriented parallel to the embryo surface and centromeres converge into a small region as they are pulled by the mitotic spindles. By interphase, chromosomes rotate to recover the upright centromere–telomere orientation. Based on analyses of mitosis in living embryos, the durations of prometaphase, metaphase, and anaphase are ~2, 3, and 1.7 min, respectively, while the total duration of mitotic cycle is 22 min at 23°C in the 13th nuclear cycle (similar values are reported in Minden et al., 1989). Lower panel is a schematic diagram of chromosomes (*lightly shaded*; *darkly shaded circles*, centromeres), nuclear envelope (*cross-hatched*), and mitotic spindle (*thick lines*) during prometaphase. The top portion of the nuclear envelope breaks down first; mitotic spindle is formed through the partially degraded nuclear envelope. Chromosomes are packed into the metaphase plate as a wave from the top to the bottom as the nuclear envelope sequentially breaks down.

We thank Dr. M. Gatti for providing his cytological maps of *Drosophila melanogaster* diploid chromosomes, Hans Chen for computer software development, Jonathan Minden for his help in microinjecting embryos, and Michael Paddy for his help in spread chromosome preparations. We also thank Mary Rykowski, Hirohisa Masuda, Tokuko Haraguchi, and Elizabeth Blackburn for critical reading of the manuscripts.

This work was supported by grants from National Institute of Health to J. W. Sedat (GM-25101) and D. A. Agard (GM-31627). J. W. Sedat and D. A. Agard are Howard Hughes Investigators. D. A. Agard is also a National Science Foundation Presidential Young Investigator. Y. Hiraoka was supported by Damon Runyon-Walter Winchell Cancer Research Fund Fellowship DRG903.

Received for publication 16 July 1990 and in revised form 5 September 1990.

References

Agard, D. A. 1984. Optical sectioning microscopy: cellular architecture in three dimensions. *Annu. Rev. Biophys. Bioeng.* 13:191–219.

Agard, D. A., and J. W. Sedat. 1983. Three-dimensional architecture of a polytene nucleus. *Nature (Lond.).* 302:676–681.

Agard, D. A., Y. Hiraoka, and J. W. Sedat. 1988. Three-dimensional light microscopy of diploid Drosophila chromosomes. *Cell Motil. Cytoskeleton.* 10:18–27.

Agard, D. A., Y. Hiraoka, P. Shaw, and J. W. Sedat. 1989. Fluorescence microscopy in three dimensions. *Methods Cell Biol.* 30:353–377.

Aikens, R. S., D. A. Agard, and J. W. Sedat. 1989. Solid-state imagers for microscopy. *Methods Cell Biol.* 29:291–313.

Anderson, K. V., and J. A. Lengyel. 1979. Rates of synthesis of major classes of RNA in Drosophila embryos. *Dev. Biol.* 70:217–231.

Ashley, T., and E. B. Wagenaar. 1974. Telomeric association of gametic and somatic chromosomes in diploid and autotetraploid Ornithogalum virens. *Can. J. Genet. Cytol.* 16:61–76.

Avivi, L., and M. Feldman. 1980. Arrangement of chromosomes in the interphase nucleus of plants. *Hum. Genet.* 55:281–295.

Belmont, A. S., J. W. Sedat, and D. A. Agard. 1987. A three-dimensional approach to mitotic chromosome structure: Evidence for a complex hierarchical organization. *J. Cell Biol.* 105:77–92.

Belmont, A. S., M. B. Braunfeld, J. W. Sedat, and D. A. Agard. 1989. Large-scale chromatin structural domains within mitotic and interphase chromosomes in vivo and in vitro. *Chromosoma (Berl.).* 98:129–143.

Blackburn, E. H. 1990. Telomeres: structure and synthesis. *J. Biol. Chem.* 265:5919–5921.

Blackburn, E. H., and J. W. Szostak. 1984. The molecular structure of centromeres and telomeres. *Annu. Rev. Biochem.* 53:163–194.

Brakenhoff, G. J., E. A. van Spronsen, H. T. van der Voort, and N. Nanninga. 1989. Three-dimensional confocal microscopy. *Methods Cell Biol.* 30: 379–398.

Chaly, N., and D. L. Brown. 1988. The prometaphase configuration and chromosome order in early mitosis. *J. Cell Sci.* 91:325–335.

Chen, H., J. Sedat, and D. A. Agard. 1989. Manipulation, display, and analysis of three-dimensional biological images. *In* The Handbook of Biological Confocal Microscopy. J. Pawley, editor. IMP Press, Madison, Wisconsin. 127–135.

Comming, D. E. 1980. Arrangement of chromatin in the nucleus. *Hum. Genet.* 53:131–143.

Cremer, T., C. Cremer, H. Baumann, E.-K. Luedke, K. Sperling, V. Teuber, and C. Zorn. 1982. Rabl's model of the interphase chromosome arrangement tested in chinese hamster cells by premature chromosome condensation and laser-UV microbeam experiments. *Hum. Genet.* 60:46–56.

Dancis, B. M., and G. P. Holmquist. 1979. Telomere replication and fusion in eukaryotes. *J. Theor. Biol.* 78:211–224.

Ellison, J. R., and G. C. Howard. 1981. Non-random position of the AT rich DNA sequences in early embryos of Drosophila virilis. *Chromosoma (Berl.).* 83:555–561.

Fay, F. S., W. Carrington, and K. E. Fogarty. 1989. Three-dimensional molecular distribution in single cells analysed using the digital imaging microscope. *J. Microsc.* 153:133–149.

Foe, V. E., and B. M. Alberts. 1983. Studies of nuclear and cytoplasmic behavior during the five mitotic cycles that precede gasturation in Drosophila embryogenesis. *J. Cell Sci.* 61:31–70.

Foe, V. E., and B. M. Alberts. 1985. Reversible chromosome condensation induced in Drosophila embryos by anoxia: visualization of interphase nuclear organization. *J. Cell Biol.* 100:1623–1636.

Freeman, M., C. Nusslein-Volhard, and D. M. Glover. 1986. The dissociation of nuclear and centrosomal division in gnu, a mutation causing giant nuclei in Drosophila. *Cell.* 46:457–468.

Fuchs, J.-P., H. Giloh, C.-H. Kuo, H. Saumweber, and J. W. Sedat. 1983. Nuclear structure: determination of the fate of the nuclear envelope in Drosophila during mitosis using monoclonal antibodies. *J. Cell. Sci.* 64: 331–349.

Fussel, C. P. 1975. The position of interphase chromosomes and late replicating DNA in centromere and telomere regions of *Allium cepa L. Chromosoma (Berl.).* 50:201–210.

Fussel, C. P. 1984. Interphase chromosome order: a proposal. *Genetica (The Hague).* 62:193–201.

Gatti, M., and S. Pimpinelli. 1983. Cytological and genetic analysis of the Y chromosome of Drosophila melanogaster. I. Organization of the fertility factors. *Chromosoma (Berl.).* 88:349–373.

Gatti, M., S. Pimpinelli, and G. Santini. 1976. Characterization of Drosophila heterochromatin. I. Staining and decondensation with Hoechst 33258 and quinacrine. *Chromosoma (Berl.).* 57:351–375.

Gelbart, W. M. 1982. Synapsis-dependent allelic complementation at the decapentaplegic gene complex in Drosophila melanogaster. *Proc. Natl. Acad. Sci. USA.* 79:2636–2640.

Glover, D. M. 1989. Mitosis in Drosophila. *J. Cell Sci.* 92:137–146.

Green, M. M. 1959. Spatial and functional properties of pseudoalleles at the white locus in Drosophila melanogaster. *Heredity.* 13:303–315.

Gurley, L. R., J. A. D'Anna, S. S. Barham, L. L. Deaven, and R. A. Tobey. 1978. Histone phosphorylation and chromatin structure during mitosis in Chinese hamster cells. *Eur. J. Biochem.* 84:1–15.

Halfer, C. 1981. Interstain heterochromatin polymorphisms in Drosophila melanogaster. *Chromosoma (Berl.).* 84:195–206.

Heald, R., and F. McKeon. 1990. Mutations of phosphorylation sites in lamin A that prevent nuclear lamina disassembly in mitosis. *Cell.* 61:579–589.

Hiraoka, Y., J. W. Sedat, and D. A. Agard. 1987. The use of a charge-coupled device for quantitative optical microscopy of biological structures. *Science (Wash. DC.).* 238:36–41.

Hiraoka, Y., J. S. Minden, J. R. Swedlow, J. W. Sedat, and D. A. Agard. 1989. Focal points for chromosome condensation and decondensation from three-dimensional in vivo time-lapse microscopy. *Nature (Lond.).* 342: 293–296.

Hiraoka, Y., J. W. Sedat, and D. A. Agard. 1990. Determination of three-dimensional imaging properties of a light microscope system: Partial confocal behavior in epifluorescence microscopy. *Biophys. J.* 57:325–333.

Hochstrasser, M., D. Mathog, Y. Gruenbaum, H. Saumweber, and J. W. Sedat. 1986. Spatial organization of chromosomes in the salivary gland nuclei of *Drosophila melanogaster. J. Cell Biol.* 102:112–123.

Holmquist, G. 1975. Hoechst 33258 fluorescent staining of Drosophila chromosomes. *Chromosoma (Berl.).* 49:333–356.

Holmquist, G. P., and B. Dancis. 1979. Telomere replication, kinetochore organization, and satellite DNA evolution. *Proc. Natl. Acad. Sci. USA.* 76:4566–4570.

Jack, J. W., and B. H. Judd. 1979. Allelic pairing and gene regulation: a model for the zeste-white interaction in Drosophila melanogaster. *Proc. Natl. Acad. Sci. USA.* 76:1368–1372.

Karr, T. L., and B. M. Alberts. 1986. Organization of the cytoskeleton in early *Drosophila* embryos. *J. Cell Biol.* 102:1494–1509.

Kaufmann, B. P. 1934. Somatic mitoses of Drosophila melanogaster. *J. Morphol.* 56:125–155.

Kilmartin, J. V., B. Wright, and C. Milstein. 1982. Rat monoclonal antibodies derived by using a new nonsecreting rat cell line. *J. Cell Biol.* 93:576–582.

Kuo, C. H., H. Giloh, A. B. Blumenthal, and J. W. Sedat. 1982. A library of monoclonal antibodies to nuclear proteins from Drosophila melanogaster embryos. *Exp. Cell Res.* 142:141–154.

Lewis, E. B. 1954. The theory and application of a new method of detecting chromosomal rearrangements in Drosophila melanogaster. *Am. Nat.* 88: 225–239.

Luby-Phelps, K., D. L. Taylor, and F. Lanni. 1986. Probing the structure of cytoplasm. *J. Cell Biol.* 102:2015–2022.

Mathog, D. 1985. Light microscope based analysis of three-dimensional structure: applications to the study of Drosophila salivary gland nuclei. II. Algorithms for model analysis. *J. Microsc.* 137:253–273.

Mathog, D., M. Hochstrasser, Y. Gruenbaum, H. Saumweber, and J. W. Sedat. 1984. Characteristic folding pattern of the polytene chromosomes in Drosophila salivary gland nuclei. *Nature (Lond.).* 308:414–421.

Matthews, H., and E. Bradbury. 1978. The role of histone H1 phosphorylation in the cell cycle: turbidity studies of H1-DNA interactions. *Exp. Cell Res.* 111:343–351.

Minden, J. S., D. A. Agard, J. W. Sedat, and B. M. Alberts. 1989. Direct cell linage analysis in Drosophila melanogaster by time-lapse, three-dimensional optical microscopy of living embryos. *J. Cell Biol.* 109:505–516.

Mitchinson, T. J., and J. W. Sedat. 1983. Localization of antigenic determinants in whole Drosophila embryos. *Dev. Biol.* 99:261–264.

Nurse, P. 1990. Universal control mechanism regulating onset of M-phase. *Nature (Lond.).* 344:503–508.

Oud, J. L., A. Mans, G. J. Brakenhoff, H. T. M. van der Voort, E. A. van Spronsen, and N. Nanninga. 1989. Three-dimensional chromosome arrangement of Crepis capillaris in mitotic prophase and anaphase as studied by confocal scanning laser microscopy. *J. Cell Sci.* 92:329–339.

Paddy, M. R., A. S. Belmont, H. Saumweber, D. A. Agard, and J. W. Sedat. 1990. Interphase nuclear envelope lamins form a discontinuous network in interphase nuclei which interacts with only a fraction of the chromatin in the nuclear periphery. *Cell.* 62:89–106.

Peter, M., J. Nakagawa, M. Dorée, J. C. Labbé, and E. A. Nigg. 1990. In vitro disassembly of the nuclear lamina and M phase-specific phosphorylation of lamins by cdc2 kinase. *Cell.* 61:591–602.

Pimpinelli, S., G. Santini, and M. Gatti. 1976. Characterization of Drosophila heterochromatin. II. C- and N-banding. *Chromosoma (Berl.).* 57:377–386.

Raff, J. W., and D. M. Glover. 1988. Nuclear and cytoplasmic mitotic cycles continue in Drosophila embryos in which DNA synthesis is inhibited with aphidicolin. *J. Cell Biol.* 107:2009–2019.

Rawlins, D. J., and P. J. Shaw. 1988. Three-dimensional organization of chromosomes of Crepis capillaris by optical tomography. *J. Cell Sci.* 91: 401–414.

Sullivan, W., J. S. Minden, and B. Alberts. 1990. *daughterless-abo-like*, a Drosophila maternal-effect mutation that exhibits abnormal centrosome separation during the late blastderm divisions. *Development.* In press.

Vandré, D. D., and G. G. Borisy. 1985. The interphase-mitosis transformation of the microtubule network in mammalian cells. *In* Cell Motility: Mechanism and Regulation. H. Ishikawa, S. Hatano, H. Sato, editors. University of Tokyo Press, Japan. 389–401.

Ward, G. E., and M. W. Kirschner. 1990. Identification of cell cycle-regulated phosphorylation sites on nuclear lamin C. *Cell.* 61:561–577.

Wu, C. T., and M. L. Goldberg. 1989. The Drosophila zeste gene and transvection. *Trends Genetics.* 5:189–194.

Young, B. S., A. Pession, K. L. Traverse, C. French, and M. L. Pardue. 1983. Telomere region in Drosophila share complex DNA sequences with pericentric heterochromatin. *Cell.* 34:85–94.

Zakian, V. A. 1989. Structure and function of telomeres. *Annu. Rev. Genet.* 23:579–604.

Zalokar, M., and I. Erk. 1976. Division and migration of nuclei during early embryogenesis of Drosophila melanogaster. *J. Microsc. Biol. Cell.* 25: 97–106.